Evolutionary and Deterministic Methods for Design,
Optimization and Control with Applications to Industrial and Societal Problems
EUROGEN 2005
R. Schilling, W.Haase, J. Periaux, H. Baier, G. Bugeda (Eds)

AERO-THERMAL-ELASTICITY-MATERIALS OPTIMIZATION OF COOLED GAS TURBINE BLADES: SUMMARY

George S. Dulikravich*, Thomas J. Martin, Brian H. Dennis*** and Igor N. Egorov†**

* Department of Mechanical and Materials Engineering, Florida International University,
MAIDROC Laboratory, 10555 W. Flagler St., Miami, FL 33174, U.S.A.
e-mail: dulikrav@fiu.edu Web page: http://maidroc.fiu.edu

** Pratt & Whitney Engine Company, Turbine Discipline Engineering & Optimization Group,
M/S 169-20, East Hartford, CT 06108, U.S.A.

*** Department of Mechanical and Aerospace Engineering, University of Texas at Arlington,
UTA Box 19018, 500 West First Street, Arlington, TX 76019, U.S.A.

† IOSO Technology Center, Vekovaia St., 21, Office 203, 109544, Moscow, Russia

Keywords: Multi-Objective Optimization, Hybrid Optimization, Turbomachinery Design

Abstract. *This is a summary of two papers presented at a VKI Workshop held in November of 2004. The first lecture in this two-lecture sequence provides background and general concepts. The second lecture provides practical examples. The objective of these two lectures was to provide a modular design optimization tool description that will take into account interaction of the hot gas flow-field, heat transfer in the blade material, stresses and deformations of the blades in an axial gas turbine. These methodologies should result in a multi-disciplinary design optimization tool for the entire system (a multi-stage turbine) rather than a design method for an isolated component (a single turbomachinery blade).*

The resulting benefits of using this general approach to design are:

1. *maximized efficiency and minimum size and weight of the entire multi-stage cooled gas turbine at design and a wide range of off-design conditions,*
2. *multi-stage 3-D design capability instead of an isolated blade row capability,*
3. *simultaneous account of several disciplines instead of aerodynamics alone,*
4. *ability to specify geometric, flow-field, thermal, and stress/deformation constraints,*
5. *capability to optimize thermally coated and uncoated turbine blades, and*
6. *optimized thickness distribution of blade walls and interior struts of cooling passages.*

INTRODUCTION

Modern turbomachinery rotor blades and vanes have traditionally been cooled by directing compressor bleed air through passages in the engine and into the complex serpentine-like coolant flow passages within the blades. The aerospace engineer thus encounters the conflicting goals of the internal cooling optimization paradox. The heat transfer into the turbine blade should be maximized so that the turbine inlet temperature can be increased, which is contrary to the other objective of minimizing the coolant flow rate and the coolant pressure losses in the coolant passages [8, 9]. Simultaneously, the objective is to avoid extremely large temperature gradients in order to prevent thermal stresses and thermal barrier coating spalation. Thus, the following question can be posed, *"Is it possible to design a turbine cooling scheme that simultaneously maximizes the turbine inlet temperature, minimizes the coolant requirements, and maintains its structural integrity?"*

2 OPTIMIZATION ALGORITHMS

A number of existing and emerging concepts and methodologies applicable to automatic inverse design and design optimization of arbitrary realistic 3-D configurations have been surveyed and compared in the past, with the following conclusions:

- Gradient search sensitivity-based optimization methods are very computationally intensive and unreliable for large shape optimization problems since they terminate in the nearest available local minima thus offering only minor design improvements,
- Brute force application of genetic evolution optimizers is very computationally intensive for realistic 3-D shape optimization problems that involve a number of equality constraints, and
- Adjoint operator (control theory) algorithms are too field-specific and governing equation specific, complex to understand and develop, hard to modify, and prone to local minima.

2.1 A hybrid optimization algorithm

A combination of several standard optimization algorithms with an automatic switching logic among them represents a hybrid optimizer that exploits the best features of each algorithm [5, 1]. The driven module is very often the Particle Swarm method, which often performs most of the optimization task. When certain percent of the particles find a minima (let us say, some birds already found their best nesting place), the algorithm switches automatically to the Differential Evolution method and the particles (birds) are forced to breed. If there is an improvement in the objective function, the algorithm returns to the Particle Swarm method, meaning that some other region is more likely to having a global minimum. If there is no improvement on the objective function, this can indicate that this region already contains the global value expected and the algorithm automatically switches to the BFGS method in order to find its location more precisely. In Figure 1, the algorithm returns to the Particle Swarm method in order to check if there are no changes in this location

and the entire procedure repeats itself. After some maximum number of iterations is performed (e.g., five) the process stops. In the Particle Swarm method, the probability test of the Simulated Annealing is performed in order to allow the particles (birds) to escape from local minima, although this procedure most often does not make any noticeable improvement in the method. Notice that this hybrid optimization method differs considerably from the earlier version that performed automatic switching among six classical optimization modules.

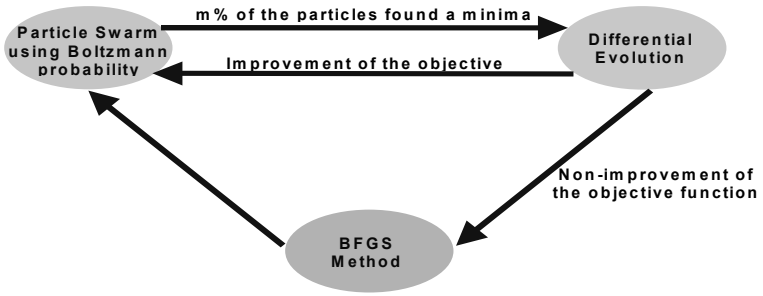

Figure 1. Global procedure for our new hybrid optimization method [1].

2.2 Method of Indirect Optimization based upon Self-Organization (IOSO) and evolutionary simulation principles [6]

The IOSO method is a constrained optimization algorithm based on self-adapting response surface methods and evolutionary simulation principles. Each iteration of IOSO consists of two steps. The first step is the creation of a local approximation of the objective functions. Each iteration in this step represents a decomposition of an initial approximation function into a set of simple approximation functions (Fig. 2). The final response function is a multi-level graph (Fig. 3). The second step is the optimization of this approximation function. This approach allows for self-corrections of the structure and the parameters of the response surface approximation to make it more accurate in regions of the design space that promise rapid convergence.

The obtained response functions are used in the procedures of multi-level optimization with the adaptive changing of the simulation level within the frameworks of both single and multiple disciplines of the object analysis. During each iteration of IOSO, the optimization of the response function is performed only within the current search area. This step is followed by a direct call to the mathematical analysis model for the obtained point. During the IOSO operation, the information concerning the behavior of the objective function in the vicinity of the extremum is stored, and the response function is made more accurate only for this search area. Thus, a series of approximation functions for a particular objective of optimization is built at each iteration. These functions differ from each other according to both structure and definition range. The subsequent optimization of these approximation functions allows us to determine a set of vectors of optimized variables, which are used for the computation of optimization objectives on a parallel computer.

For a basic parallel IOSO algorithm, the following steps are carried out:

1. Generate a group of designs based on a design of experiments (DOE) method;
2. Evaluate the designs in parallel with the analysis code;
3. Build initial approximation based on the group of evaluated designs;
4. Use stochastic optimization method to find the minimum of the approximation;
5. Do adaptive selection of current extremum search area;
6. Generate a new set of designs in current extremum search area using DOE;
7. Evaluate the new set of designs in parallel with the analysis code;
8. Update the approximation with newly obtained result;
9. Goto 4, unless termination criteria is met.The distinctive feature of IOSO algorithm is an extremely low number of trial points to initialize the algorithm (30-50 points for the optimization problems with nearly 100 design variables). In addition, IOSO was successfully applied to problems with hundreds of design variables and a large number of constraints and objective functions.

If a large number of processors are available, the optimizer can use all of them by running several simultaneous parallel analyses to evaluate several candidate design configurations. For this research an optimization communication module was developed using the MPI library that utilizes this multi-level hierarchy of parallelism. This module can be used with any parallel optimization method including genetic algorithm (GA) and IOSO algorithm.

Multi-objective optimization algorithms have been successfully applied in a number of engineering disciplines. Such algorithms are needed to solve actual multi-disciplinary industrial application design problems having hundreds of highly constrained design variables and several simultaneous objectives. In multi-objective optimization we strive to compute the group of the *not-dominated* solutions, which is known as the Pareto optimal set, or Pareto front. These are the feasible solutions found during the optimization that cannot be improved for any one objective without degrading another objective.

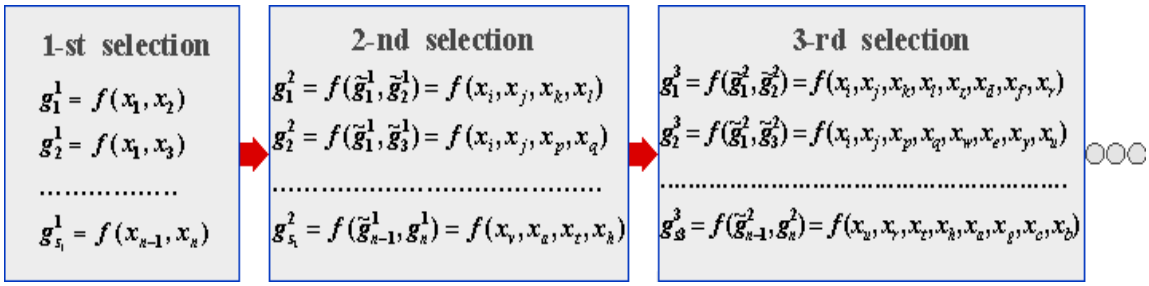

Figure 2. A decomposition of an initial approximation function (a response surface) into a set of simple approximation functions.

We have found that IOSO multi-objective constrained optimization algorithm is superior to any other currently available multi-objective optimizer. The effectiveness of IOSO optimization procedure has been demonstrated with the examples of car engine exhaust toxicity minimization (3 variables, 4 objectives), optimal control laws for the power plant of a short take-off and vertical landing aircraft for its take-off mode (50 variables, 2 objectives),

the preliminary solution of the problem of a multi-stage axial compressor optimization aimed at its efficiency maximization (42 variables, 2 objectives), and optimization of concentration of alloying element in a minimum expensive superalloy for maximum strength, time-to-rupture, and temperature (14 variables, 10 objectives) [7].

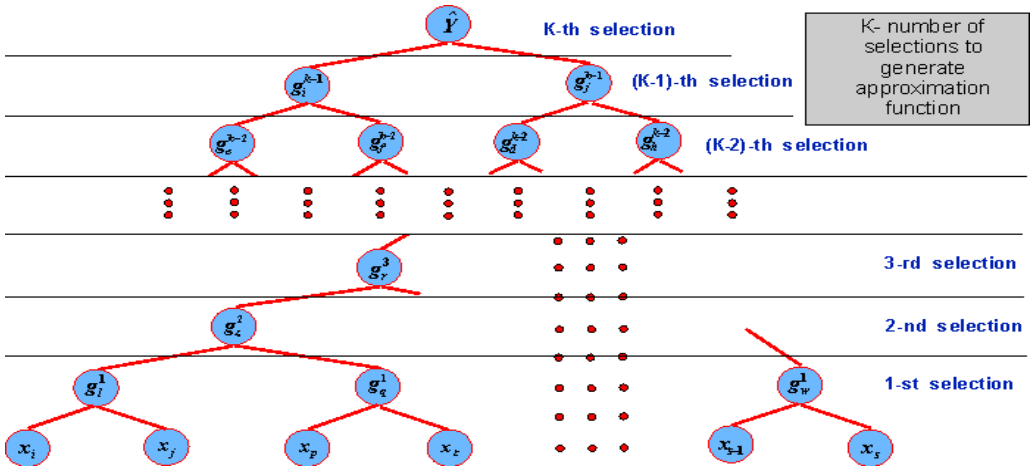

Figure 3. The final response function is a multi-level graph

3 EXAMPLES OF DESIGN OPTIMIZATION

3.1 Multi-objective optimization of airfoil cascades for minimum loss, maximum loading, and maximum gap-to-chord ratio [4]

This work illustrates an automatic multi-objective design optimization of a two-dimensional airfoil cascade row having a finite number of airfoils. The objectives were to simultaneously minimize the total pressure loss, maximize total aerodynamic loading (force tangent to the cascade), and minimize the number of airfoils in the finite cascade row. The constraints were: fixed mass flow rate, fixed axial chord, fixed inlet and exit flow angles, fixed blade cross-section area, minimum allowable thickness distribution, minimum allowable lift force, and a minimum allowable trailing edge radius. This means that the entire airfoil cascade shape was optimized including its stagger angle, thickness, curvature, and solidity. The *multi*-objective constrained optimization algorithm used in this work was IOSO. The airfoil shape was defined with the following nine parameters: the tangential and axial chord, the inlet and exit half wedge angle, the inlet and outlet airfoil angle, the throat, unguided turning angle, and the leading and trailing edge radii. One of these parameters (axial chord) was kept fixed. The airfoil shape was allowed significant additional flexibility by adding a continuous arbitrary perturbation in addition to the original nine parameters. This shape perturbation was modeled with a B-spline that had eight control vertices thus resulting in a total of 9 + 8 = 17 design variables plus one additional variable for the number of airfoils in a

finite length cascade. Thus, there were 18 design variables in this case. With these conditions we defined the following 3 objectives (Table 1) and the 5 nonlinear constraints (Table 2) for a VKI high subsonic exit flow axial turbine cascade. The constraints were incorporated in the objective functions via penalty formulation.

	OBJECTIVES
MAXIMIZE	Total loading force
MINIMIZE	Total pressure loss
MINIMIZE	Number of airfoils

Table 1. Simultaneous objectives in the multi-objective constrained optimization

CONSTRAINTS	Values
Total loading	> 186599 N
Mass flow rate (per unit span)	= 384 kg m^{-1} s^{-1}
Exit flow angle	= -70°
Airfoil cross-section area	= 108.8 mm^2
Airfoil trailing edge radius	= 0.5 mm

Table 2. Inequality and equality constraints used

	VKI	No.1	No.3	No.6
Total pressure loss, Pa	103078	95164	97050	95012
Total loading, N	186599	189359	196778	193228
Number of airfoils	45	44	46	45

Table 3. A comparison of the three objectives achieved by the original VKI cascade and the three prominent cascades obtained with our multi-objective constrained optimization.

The resulting hint of a Pareto front is depicted in Fig. 4 and shapes of the resulting airfoils are shown in Fig. 5. Cascade No.1 offers reduction of 7% in total pressure loss, needs 1 airfoil less than the VKI cascade, and generates about 1% higher total loading. Cascade No.3 offers reduction of 5% in total pressure loss, need 1 more airfoil than the VKI cascade, and generates about 6% higher total loading. Cascade No.6 offers reduction of 7% in total pressure loss, need the same number of airfoils as the VKI cascade, and generates about 4% higher total loading. This means that it is possible to design turbomachinery blade rows that will have simultaneously lower total pressure loss, higher total loading, and fewer blades while preserving some of the same features of the original blade rows (inlet and exit flow angles, total mass flow rate, blade cross-section area, and trailing edge radius). All computations were performed on our 32 node distributed memory parallel computer with 400 MHz Pentium II processors and a total of 8GB RAM. Each call to IOSO consumed a negligible fraction of time compared to each call to the flow-field analysis code which consumed about 15 minutes on a single processor.

The entire optimization procedure required a total of 5611 analysis calls to the 2-D flow-field analysis code in order to find enough points in the feasible region having relative errors in equality constraints less than one percent. Notice that the original VKI cascade already had a very high efficiency since it was designed by expert designers using an inverse shape design method.

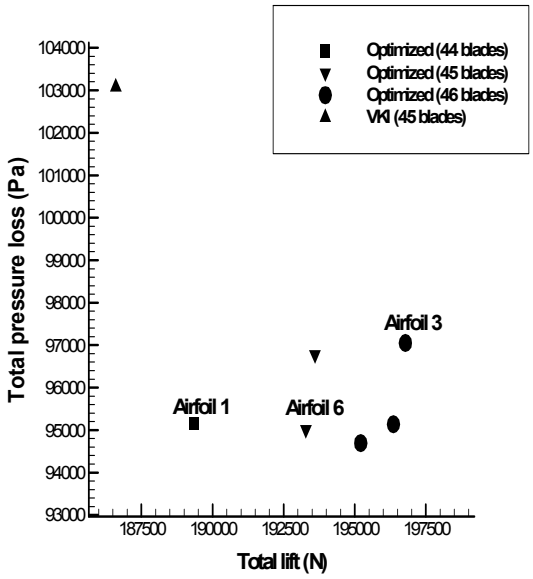

Figure 4. Comparison of total pressure loss generated versus total loading produced for various numbers of airfoils for optimized airfoil cascades and the VKI airfoil cascade.

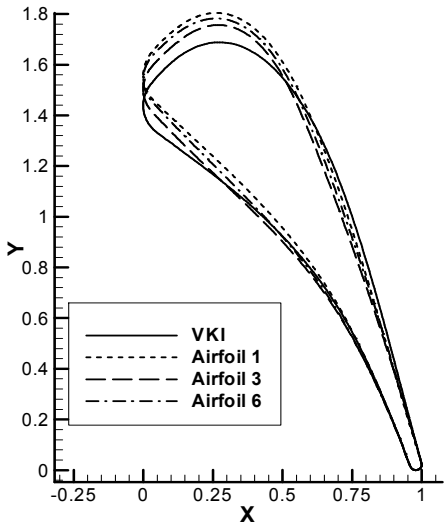

Figure 5. Comparison of three optimized airfoil cascades [4] against the original VKI airfoil cascade.

3.2 Thermal optimization of blades with a large number of cooling passages [2]

The objective here is to minimize the total amount of heat transferred to the vane (integrated heat flux on the hot surface of the vane) while maintaining a maximum temperature, T_{max}, which is lower than the maximum allowable temperature, T_{allow}. This objective indirectly minimizes the amount of coolant required to cool the vane. A numerical heat conduction analysis within the vane material is used to compute the objective and the temperature constraint. Instead of a fully 3-D conjugate heat transfer analysis or a quasi 3-D conjugate heat transfer analysis of each candidate vane configuration, heat convection boundary conditions were used to simulate the presence of coolant and hot gas. This approach includes a very approximate treatment of the fluid mechanics and excludes treatment of thermo-elasticity. The objective function is computed by integrating heat flux across the vane outer surface. There are two inequality constraints:

$$G_1 = \frac{T_{allow} - T_{max}}{T_{allow}} \qquad G_2 = \sum_{i=1}^{nholes} C_i \tag{1}$$

where *nholes* is the number of passages and C_i is a positive number when the distance between passage *i* and another passage is less than a specified distance. Otherwise the value of C_i is zero. The first constraint is necessary so that the maximum temperature in the vane material is always below the maximum allowed temperature. The second constraint is needed to insure that the optimizer only searches for valid geometries. The constraints are satisfied if $G_1 \le 0.0$ and $G_2 \le 0.0$.

The outer vane shape is considered to be fixed and to be provided by the user at the beginning of the design optimization. Presumably, this is the vane shape that has already been optimized for its aerodynamic performance. The design variables include the radius of each circular cross-section cooling passage, r_i, and position of each passage center, $<x_i,y_i>$, in the vane cross-section. The passage centers are allowed to move normal and tangential to the outer contour of the blade within a specific region as shown in Figure 6. For 30 cooling passages, this parameterization leads to a total 90 design variables. A triangular surface mesh and a tetrahedral volume mesh were generated automatically for each candidate design. The mesh generator did an adequate job of placing enough points between the passages and the vane surface, even when the passages were very close to the surface. A typical mesh had around 80,000 nodes.

This design optimization problem was solved using both parallelized GA (PGA) and IOSO. The same initial design was given to both optimizers at the start of each run.

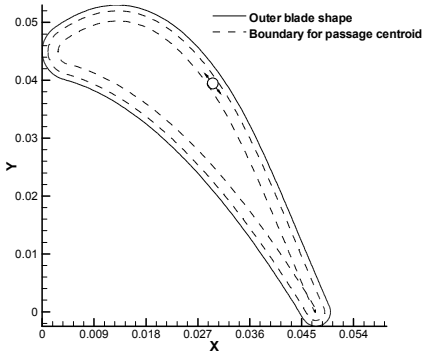

Figure 6. Region where coolant passage centers are allowed [2].

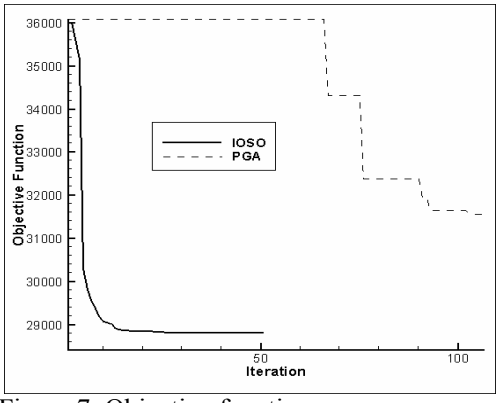

Figure 7. Objective function convergence history [2] with GPA and IOSO optimizers.

For both PGA and IOSO method, 40 configurations of cooling holes were analyzed simultaneously per iteration. Each finite element heat conduction analysis used 2 processors. The following PGA parameters were used: 5.0 percent mutation rate, 50.0 percent chance of uniform crossover, 7 bit binary encoding for y_i and 5 bit encoding for x_i, r_i. A typical design optimization can be completed within a few hours using an inexpensive cluster of personal computers. The convergence history (Fig. 7) shows that for this example the IOSO method outperforms the PGA method. Both IOSO and PGA methods reduced the total heat flux from the initial design as shown in Table 4. The IOSO optimization method was found to produce

better results with fewer iterations than the PGA method. The IOSO method is also more robust and easier to use since it requires fewer tuning parameters than the PGA method. Specifically, one can see (Fig. 8) that the topology of the passages is slightly different between the two best designs. The result of the PGA is clearly at a local optimum since some passages are clustered too closely together near the leading and trailing edge creating overcooled areas. The passage size and position for the IOSO result is more uniform than the PGA result. More iterations and more fine-tuning of control parameters, including increasing the selection pressure, could improve the PGA result.

Result	Initial guess	PGA best design	IOSO best design
nholes	30	30	30
T_{max}	892.6 ^{o}C	899.1 ^{o}C	902.3 ^{o}C
Q (Watts)	36099.8 W	31563.0 W	28808.2 W

Table 4: Optimization results for an internally cooled vane with 30 round holes.

The best possible design could be achieved if the entire outer surface temperature would be equal to T_{allow}. In this case, the integrated heat flux would be only 19830.0 W. However, a perfect design is not achievable due to the limitations of the geometric parameterization. The next step towards a complete automatic design system should be to add 3-D fluid mechanics analysis codes and 3-D thermoelasticity analysis thus providing a fully 3-D conjugate analysis environment. However, this would then increase computing time by an order of magnitude.

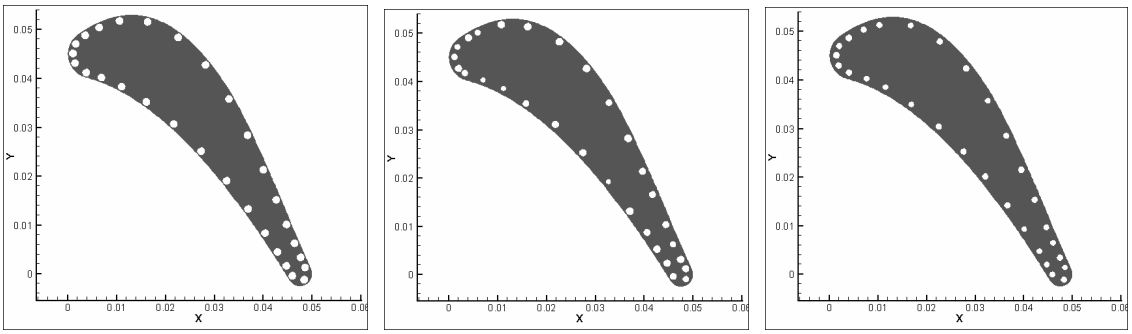

Figure 8. Cooling passages for initial design (left), PGA best design (middle), and IOSO best design (right) for a case with 30 cooling passages [2].

3.3 Thermo-elasticity optimization of 3-D serpentine cooling passages [3]

An automatic design algorithm for parametric shape optimization of three-dimensional cooling passages inside axial gas turbine blades has been developed. The outer blade geometry was created by generating a series of two-dimensional turbine airfoils and stacking the sections along the *z*-axis. Smooth serpentine passage configurations were considered. The geometry of the blade and the internal serpentine cooling passages were parameterized using surface patch analytic formulation [11], which provides very high degree of flexibility, second

order smoothness, a minimum number of parameters, and guarantees minimum wall thickness. All together a total of 42 continuous design variables were used to uniquely describe a design [3].

A parallelized 3-D thermoelasticity finite element method (FEM) computer code was used to perform automatic thermal and stress analysis of different blade configurations. The root section of the geometry was set to zero displacement while the blade and inner shroud were left free to deform. In this simplified problem the aerodynamic loads were not included. As for thermal boundary conditions, the outer surface of the blade and top surface of inner shroud were set to convection boundary conditions which require the specification of the convection coefficient, h_B, and the hot gas bulk temperature, T_B. Convection boundary conditions were also applied to the coolant passage surface inside the blade using h_C and T_C. All other surfaces were assumed thermally insulated. The objective of the optimization was to make stresses throughout the blade as uniform as possible. Constraints were that the maximum stress and temperature at any point in the blade were less than the maximum allowable values. IOSO optimizer and a parallel genetic algorithm (PGA) were used to solve this problem while running on an inexpensive distributed memory parallel computer based on an older PC cluster with 54 Pentium II 400 MHz processors. For this research an optimization communication module was developed using the MPI library that utilizes this multilevel hierarchy of parallelism. This module can be used with any parallel optimization method including PGA and IOSO algorithms.

A total of 12 analyses were performed per iteration for IOSO method. For PGA, 36 designs were evaluated per generation. For both cases each parallel thermoelastic FEM analysis used 4 processors. A typical analysis mesh contained over 150,000 degrees of freedom and required 4 minutes to complete a full thermoelasticity analysis. A converged result was found by the IOSO optimizer in 70 iterations after consuming approximately 12 hours of total computer time. For PGA, the total computer time was more than 30 hours. The PGA run was terminated before a converged result was found.

The convergence history for the objective function for both PGA and IOSO is shown in Figure 9. For all designs the stress constraint was satisfied. However, the initial design violated the temperature constraint so the optimizer had to first determine a feasible design. The convergence history for the temperature constraint function is shown in Figure 10. This figure shows that a feasible region was found at iteration 12 for IOSO and iteration 68 for PGA. For the IOSO method, after iteration 12 the best design becomes the feasible design, which is why a spike in Figure 9 occurs at iteration 12. Prior to that, only infeasible designs were found and the optimizer clearly tried to improve the objective function while searching for the feasible region. These convergence results clearly show the computational efficiency of the IOSO approach over the PGA method for this design problem.

The initial and the IOSO optimized passages configurations are shown in Figures 9. The wall near the tip corners has become much thinner in an effort to keep the temperature in those regions below the maximum allowable value. The volume of the optimized blade is slightly smaller than the initial design (Table 5), most likely due to the thinning of the walls in the tip region of the blade. The optimized design's maximum principal stress was reduced by 36 percent and its objective function reduced by 62 percent.

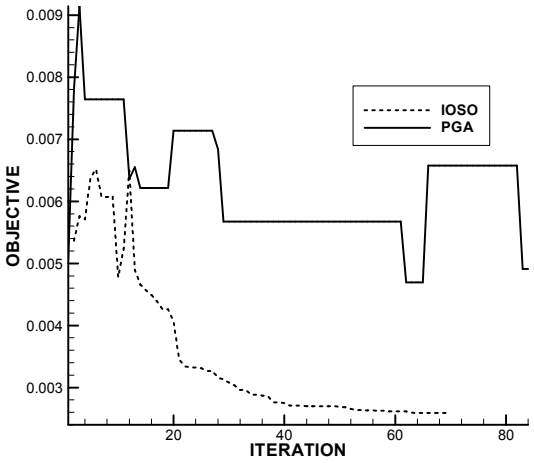

Figure 9. Objective function convergence history [3].

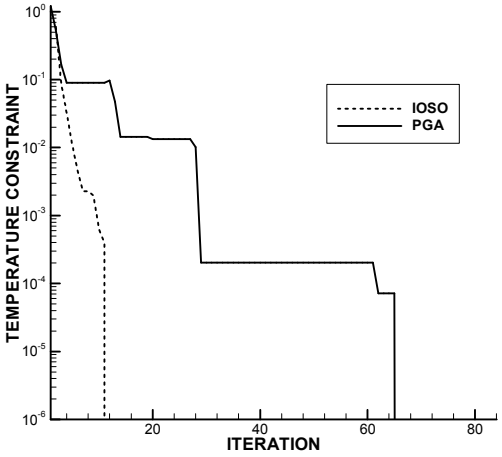

Figure 10. Temperature constraint function [3].

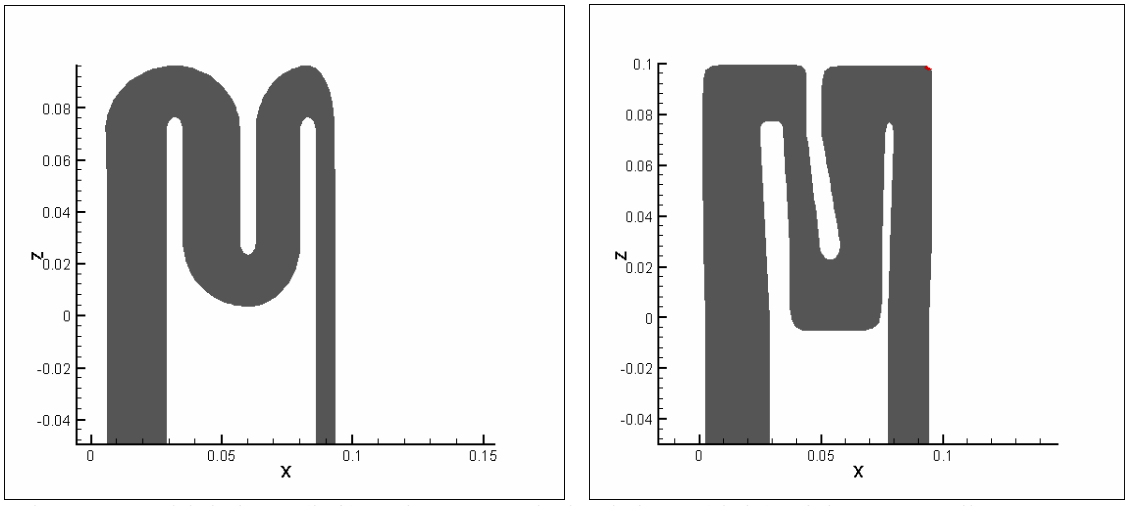

Figure 11. Initial shape (left) and IOSO optimized shape (right) of the 3-D cooling passage.

Quantity	Initial	Optimized
Maximum Temperature, T_{max}	1333.8 ^{o}C	894.6 ^{o}C
Volume	9.64×10^{-4} m^3	8.46×10^{-4} m^3
Maximum Principal Stress, $\sigma_{\max}$	668.9 MPa	425.1 MPa
Coolant bulk temperature, T_C	600.0 ^{o}C	158.0 ^{o}C
Objective function value, F	6.80×10^{-3} Pa	2.59×10^{-3} Pa

Table 5: Comparison of initial and thermo-elastically optimized cooling passage designs

The reduction in coolant temperature was necessary for the satisfaction of the maximum temperature constraint. Although the temperature difference between the coolant and outer hot gas increased, the thermal stresses actually decreased. Principal stresses on the surface of the blade with the initial shape of the coolant passage is shown in Figure 12, where the IOSO optimized coolant passage offers lower and more uniform stress field. Stress in the root of the blade is high due to the centrifugal loading and temperature gradients.

Temperature distributions for the initial design and the IOSO optimized design are shown in Figures 13. The temperature distribution on the surface of the IOSO optimized blade is considerably lower and smoother compared with that of the initial design.

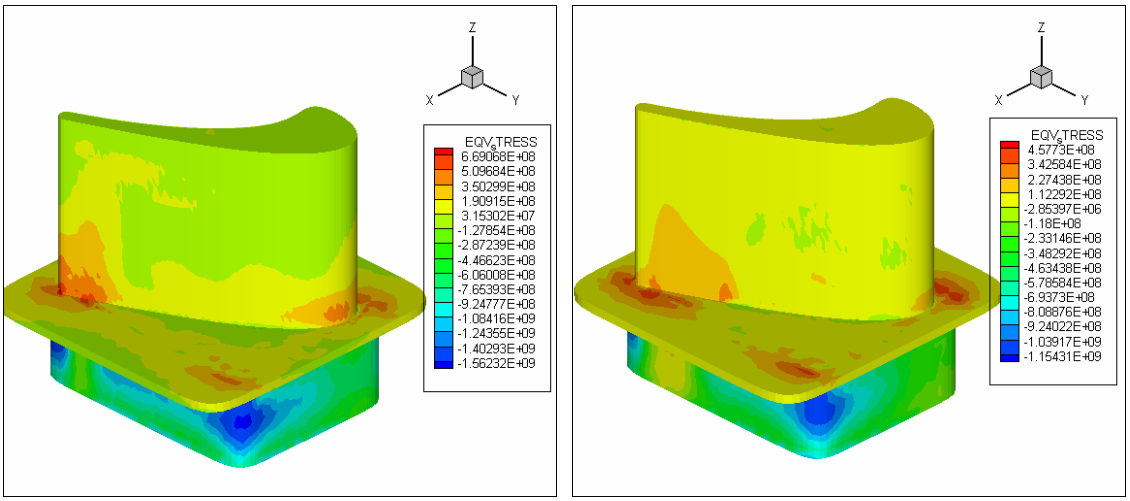

Figure 12. Principal stress contours for initial (left) and IOSO optimized design (right).

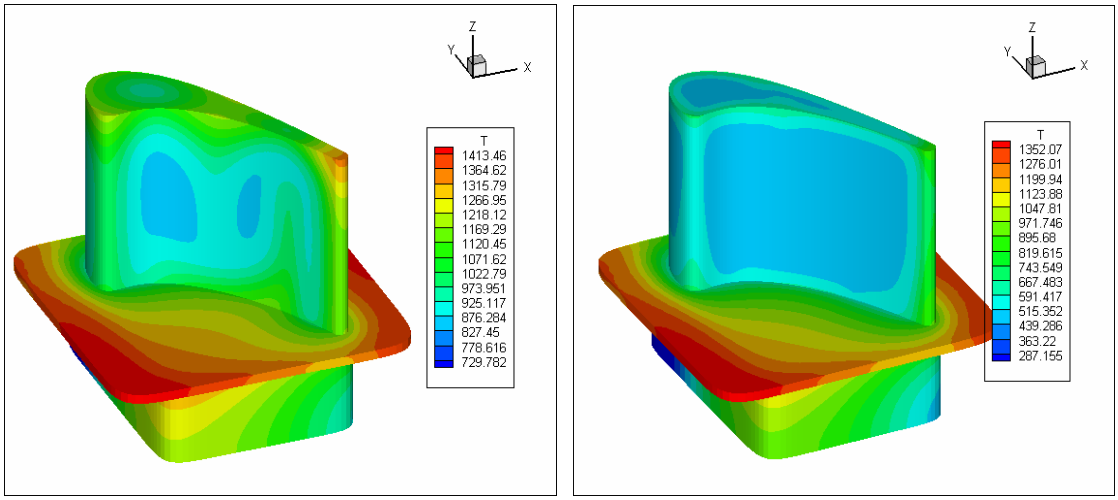

Figure 13. Surface temperature field on pressure side for the initial cooling passage shape (left) and for IOSO optimized design of 3-D cooling passage (right).

3.4 Preliminary aerodynamic optimization of a multi-stage axial gas turbine [10]

We have recently developed [10, 5] a system for preliminary design optimization of geometric and flow-field parameters of multi-stage transonic axial flow turbines at nominal and off-design conditions. It was found that by varying at least seventeen variables (eight geometric and nine flow-field parameters) per each turbine stage, it is possible to evaluate an optimal radial distribution of flow parameters at inlet and outlet of each blade row and an optimal shape of hub and shroud. The optimized solution gives the maximum efficiency of the multi-stage axial turbine. The design system has been demonstrated on a well-documented set of experimental data for a one-stage uncooled transonic axial gas turbine. The comparison of computed performance of initial and optimized designs shows significant improvement in the optimized multi-stage efficiency (Fig. 14) and reduction of entropy generation in multi-stage turbomachinery. The entire design optimization process was found to be computationally quite feasible consuming 0.75 hours on a single processor SGI R10000 workstation. Such extraordinary speed of execution was possible mainly because of the use of a highly accurate through-flow metamodel instead of the complete Navier-Stokes 3-D rotor-stator unsteady compressible turbulent flow-field analysis code.

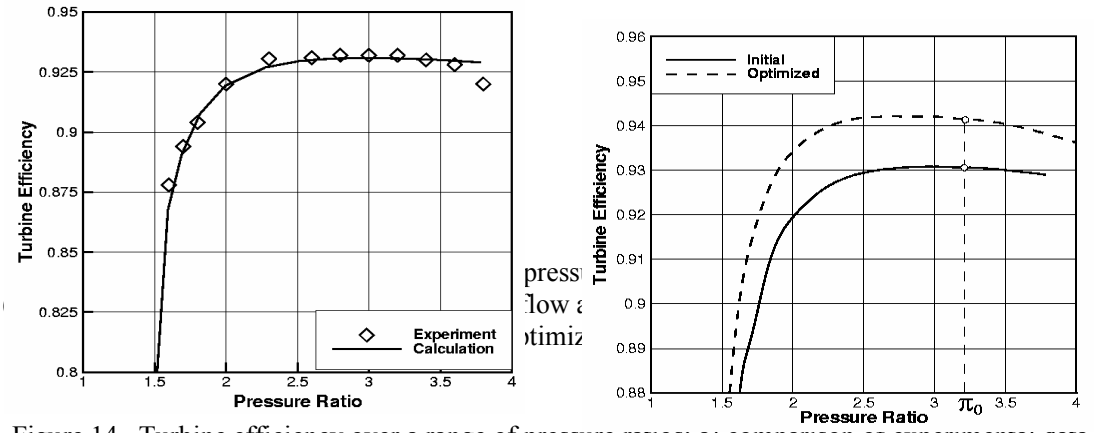

Figure 14. Turbine efficiency over a range of pressure ratios: a) comparison of experimental data (symbols) and analysis using an axisymmetric flow analysis with losses model, b) comparison with results obtained after performing optimization with a hybrid optimizer [10].

3.5 Aero-thermo-structural optimization of coolant networks in turbine blades [8,9]

A parametric computer model of the 3-D internal cooling network (Figs. 15 and 16) was combined with a boundary element computer program to solve the steady-state non-linear conjugate heat transfer in internally cooled and thermal barrier-coated turbine blades. This fully-coupled aero-thermo-fluid solution procedure was used for each design perturbation while the constrained hybrid optimizer [5] maximized the cooling effectiveness objective. The entire optimization process utilized a full week of computing time on a Sun Ultra60 requiring 630 objective function analyses and 1400 simulations of the temperature field

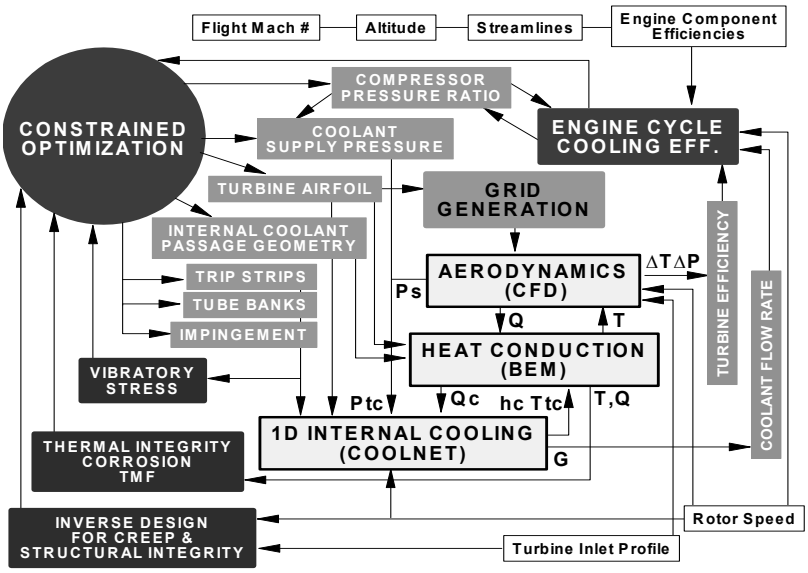

Figure 15. Flow chart for the multi-disciplinary design and optimization of internally cooled turbine airfoils.

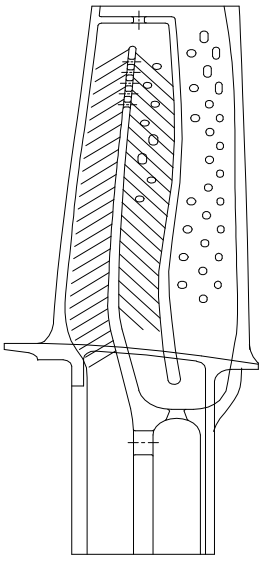

Figure 16. Cross-section schematic of the P&W F100 second rotor blade.

3.6 Design optimization of alloys for turbine blades [7]

Alloy design for critical aero-engine components is a time-consuming and expensive process. The development period prior to application in an engine is typically of the order of ten years. IOSO algorithm [6] was used in conjunction with experimental evaluations of maximum strength and time-to-rupture at high temperature to maximize these two properties in nickel based steel alloys [7]. This provides the first realistic demonstration of the entire alloy design optimization procedure and simultaneous experimental verification of this procedure. Chemical elements whose concentrations were optimized were Ni, C, Cr, Co, W, Mo, Al, Ti. Concentrations of Nb, B, Ce, Zr, Y in all sample alloys were kept constant. Two simultaneous objectives of the alloy concentration optimization were: maximize stress at 20 degrees C, and maximize time until rupture at 975 degrees C with a fixed stress of 23 kg/mm^2. We started by using 120 experimentally tested nickel based alloys and optimized concentrations of seven alloying elements in order to predict 20 new alloy compositions with potentially better properties. After experimentally testing these 20 new alloys, it was found that 7 of them indeed had superior strength and time-to-rupture at high temperature as compared to the original 120 alloys. The IOSO optimization procedure was repeated a total of four times whereby 20 new alloys were predicted and experimentally tested during each of the four design iteration cycles. The properties of the newly found alloys consistently continued improving from one iteration to the next (Figure 17). This was confirmed by experimentally evaluating these new alloys. This alloy design methodology is applicable to arbitrary alloys. It does not require any mathematical modeling of the physical properties since they are determined experimentally.

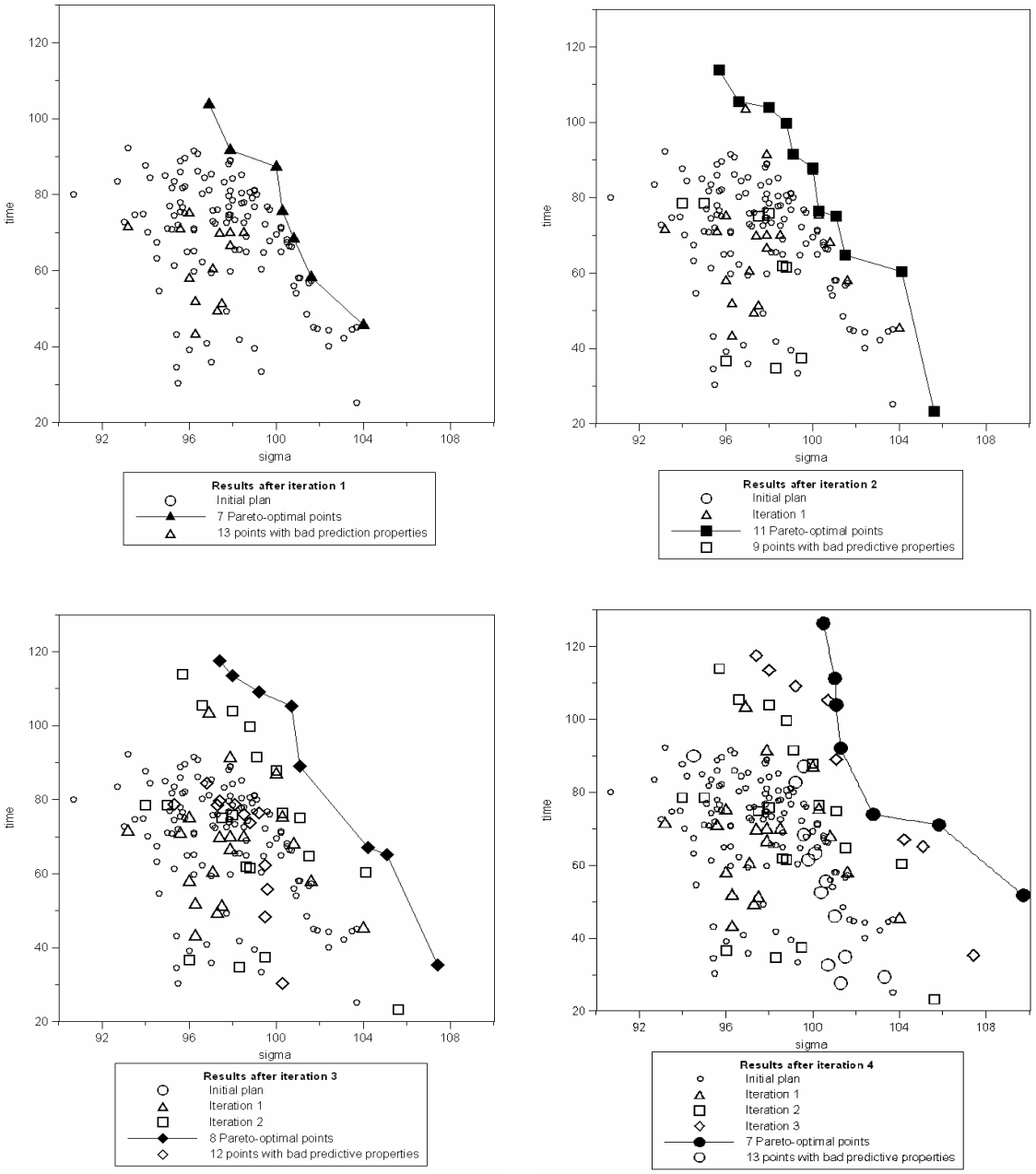

Figure 17. Experimental data for time-to-rupture at 975 degrees Celsius and stress of 23 kg/mm^2 vs. maximum tensile stress at room temperature for the 120 original Ni-base alloys (circles) and the 20 Pareto optimized new alloys (other symbols) after each of the four iterations using IOSO optimization algorithm. The experimentally confirmed Pareto optimal alloys after each optimization cycle are depicted with dark symbols.

REFERENCES

[1] Colaço, J. M., Dulikravich, G. S., Orlande, H. R. B., Martin, T. J.: Hybrid Optimization With Automatic Switching Among Optimization Algorithms, a chapter in Evolutionary Algorithms and Intelligent Tools in Engineering Optimization (eds: W. Annicchiarico, J. Périaux, M. Cerrolaza and G. Winter), CIMNE, Barcelona, Spain 2005.

[2] Dennis, B. H., Egorov, I. N., Dulikravich, G. S., Yoshimura, S.: Optimization of a Large Number of Coolant Passages Located Close to the Surface of a Turbine Blade, ASME paper GT2003-38051, ASME Turbo Expo 2003, Atlanta, GA, June 16-19, 2003.

[3] Dennis, B. H., Egorov, I. N., Sobieczky, H., Dulikravich, G. S., Yoshimura, S.: Parallel Thermoelasticity Optimization of 3-D Serpentine Cooling Passages in Turbine Blades, International Journal of Turbo & Jet-Engines, vol. 21, no. 1, 2004, pp. 57-68.

[4] Dennis, B.H., Han, Z.-X., Egorov, I.N., Dulikravich, G.S., Poloni, C.: Multi-Objective Optimization of Turbomachinery Cascades for Minimum Loss, Maximum Loading, and Maximum Gap-to-Chord Ratio, Int. J. of Turbo & Jet-Engines, Vol. 18, No. 3, pp. 201-210.

[5] Dulikravich, G. S., Martin, T. J., Dennis, B. H., Foster, N. F.: Multidisciplinary Hybrid Constrained GA Optimization, a chapter in EUROGEN '99 - Evolutionary Algorithms in Engineering and Computer Science: Recent Advances and Industrial Applications, (eds K. Miettinen, M. M. Makela, P. Neittaanmaki and J. Periaux), John Wiley & Sons, Ltd., Jyvaskyla, Finland, May 30 - June 3, 1999, pp. 231-260.

[6] Egorov, I. N.: Indirect Optimization Method on the Basis of Self-Organization, Curtin University of Technology, Perth, Australia., Optimization Techniques and Applications (ICOTA'98), vol. 2, 1998, pp. 683-691.

[7] Egorov-Yegorov, I. N., Dulikravich, G. S.: Chemical Composition Design of Superalloys for Maximum Stress, Temperature and Time-to-Rupture Using Self-Adapting Response Surface Optimization, Materials and Manufacturing Processes, 20 (3) (2005), 569-590.

[8] Martin, T. J., Dulikravich, G. S.: Analysis and Multi-disciplinary Optimization of Internal Coolant Networks in Turbine Blades", AIAA Journal of Propulsion and Power, vol. 18, no. 4, 2002, pp. 896-906.

[9] Martin, T. J., Dulikravich, G. S.: Aero-Thermo-Elastic Concurrent Design Optimization of Internally Cooled Turbine Blades, Chapter 5 in Coupled Field Problems, Series on Advances in Boundary Elements (eds: Kassab, A. J. and Aliabadi, M. H.), WIT Press, Boston, MA, 2001, pp. 137-184.

[10] Petrovic, M. V., Dulikravich, G. S., Martin, T. J.: Optimization of Multistage Turbines Using a Through-flow Code, Journal of Power and Energy, Vol. 215, Part A, 2001, pp. 559-569.

[11] Sobieczky, H., Dulikravich, G. S., Dennis, B. H.: Parameterized Geometry Formulation for Inverse Design and Optimization, 4th International Conference on Inverse Problems in Engineering: Theory and Practice (4icipe), (ed: Orlande, H. R. B.), Angra dos Reis, Brazil, May 26-31, 2002.